Literatur summary

Dienstag, 4. Mai 2021 16:19

<table>
<tr><th>Paper</th><th>Notes</th><th>What model is used?</th><th>How do they obtain the data?</th><th>On what data is the model trained?
How much?</th><th>Mono material or polymaterial?</th><th>Cone beam geometry ? (Yes/ No)</th><th>#epochs</th><th>Batch size</th><th>Optimizer</th><th>Loss</th><th>Hyperparameter</th><th>Train time</th><th>Results</th></tr>
<tr><td>2020, Ziabari et al. Beam Hardening artifact reduction</td><td></td><td>2-Models but we focus here just on the dominant one: AI-CT
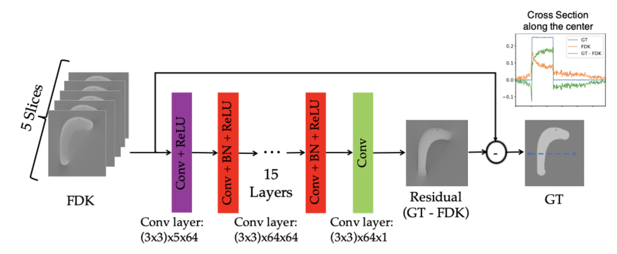

1. The schematic of AI-CT is shown in Figure 6. It consists of 17 convolutional layers with the transformation kernel of the form $(3 \times 3) \times N_{in} \times N_{out}$. Here, (3×3) represents the convolution filter size applied with N_{in} input and N_{out} output channels. Batch normalization (BN) and ReLU were applied in the middle 15 layers.</td><td>• Use CAD data to get ground truth
• Measured coefficients E_1, E_2, alpha through a fit of
$$-\log\left(\frac{I}{I_0}\right) = \left(\frac{\alpha}{1+\alpha}\mu(E_1) + \frac{1}{1+\alpha}\mu(E_2)\right) d \equiv \mu_{eff} d,$$
Onto real real data.
• Used this coefficients to simulate Cone Beam artifacts on the CAD ground truth data with the ASTRA toolbox
• Inserted cracks/ holes to test the performance of the network (not to much removement)</td><td>• Trained on noisy input slices and residual output slice (Noisy input - Ground Truth)
  • Data has extra artifacts to test perfromance
  • 5 neighbouring input slices
  • 1 middle output residual slice

• Six volumes of CT-reconstruction data
  • Splitted into patches of 256 x 256
    ○ One volume --> Many samples
  • Patch with to many background voxels is removed (average value smaller than mean of ull volume)
  • Effectivly only have of the volumes were used
    ○ 80% train
    ○ 20% validation

• No downsampling</td><td>Only trained on jet-engine turbine blades (relativly homogenous material) (Inconel738) --> Mono material</td><td>Yes</td><td>-</td><td>16</td><td>Adam</td><td>Mean squared error of residual</td><td>Lr = 0.001
Beta_1 = 0.9
Beta_2 = 0.999

Every 70 epochs learning rate reduces by factor 2
Or if validation loss increases
For three consecutive epochs</td><td>--</td><td>Computed Peak Signal to Noise ratio
$$PSNR \equiv 20\log\left(\frac{x_{GT,max}}{MSE}\right),$$
• MSE: Mean squared Error
• X_GT,max: maximal pixel value ground truth
• Did not used air voxels, only voxels within CAD model region

TABLE 1. Mean PSNR And SSIM for Reconstruction Volumes
<table><tr><th>Method</th><th>FDK, No Corr.</th><th>MBIR w/ BH Corr</th><th>MSD-Net</th><th>AI-CT</th></tr><tr><td>Avg. PSNR (dB) (Case 1)</td><td>16.42</td><td>36.52</td><td>37.24</td><td>53.11</td></tr><tr><td>Avg. PSNR (dB) (Case 2)</td><td>16.37</td><td>41.47</td><td>35.68</td><td>45.05</td></tr></table>
AI-CT does clearly outperform classical techniques (MBIR Beam hardening correction)
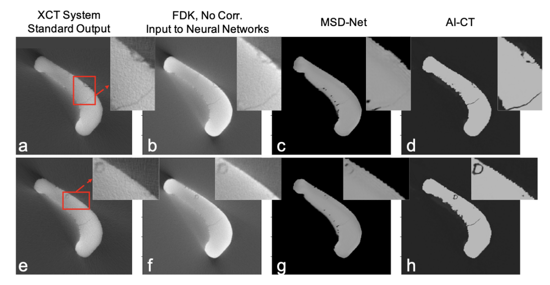

FIGURE 10. Significant performance of AI-CT in reconstruction of real data in the airfoil region. Both AI-CT and MSD-Net were trained only on synthetic data.

Cracks/ holes are also preserved!</td></tr>
<tr><td>2019, Pauwels</td><td></td><td>U-Net(CNN) from Ronnenberger et al. (2015)
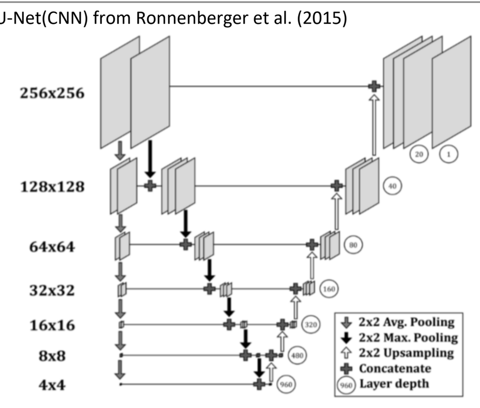

• Radiographs downsampled to 256x256 --> Later upsampling needed
• Model idea: 2 paths (contracting & symmetric expanding) --> Allows feature contraction and percise localization at the same time
• 32 797 740 network trainable parameters
3 CNNs proposed:
• $CNN_{SCAT-MONO}$: Single network for scattering &beam-hardening (1x Unet)
• Dual Network:
  ○ $CNN_{SCAT-POLY}$: 1x Unet fur Scattering which is fed then into the other
  ○ $CNN_{POLY-MONO}$: 1x Unet Beam Hardening</td><td>• Data simulation with aRTist (BAM)
• Simulations with point-shape focal spot,2.0 magnification, noiseless conditions
• 1° scan intervals
• 3 conditions simulated:
  • Polychromatic
  • Monochromatic
  • Polychromatic with MC scatter</td><td>• Radiographs as data used as input
• Output is noise artefact map
  • In the end upsample& subtract artefact map from original radiograph
• Labels were the effect(s) itself:
  • $CNN_{SCAT-MONO}$: SCAT-MONO
  • $CNN_{SCAT-POLY}$: SCAT-POLY
  • $CNN_{POLY-MONO}$: POLY-MONO
• Total Data size used:
  • 22 objects
  • 7920 radiographs per exposue (polcy, mono, poly-scat)
  • Total: 23760 radiographs
• Train data:
  • 20 objects data
  • 7200 images
• Validation data:
  • 720 radiographs
  • 2 objects</td><td>Polymaterial: "titanium, aluminium, iron"</td><td>-</td><td>160</td><td>16</td><td>Adam with AMSgrad</td><td>Mean squared error</td><td>Initial lr: 0.001</td><td><100s per epoch, High throughput for inference ~20ms/ radiograph</td><td><table><tr><th></th><th></th><th>$CNN_{SCAT-MONO}$</th><th>$CNN_{SCAT-POLY}$</th><th>$CNN_{POLY-MONO}$</th></tr><tr><td>Training</td><td>RMSE</td><td>19.7</td><td>6.7</td><td>17.8</td></tr><tr><td></td><td>$ACC_{1\%}$</td><td>0.262</td><td>0.672</td><td>0.553</td></tr><tr><td></td><td>$ACC_{5\%}$</td><td>0.682</td><td>0.997</td><td>0.913</td></tr><tr><td></td><td>$ACC_{10\%}$</td><td>0.818</td><td>1.000</td><td>0.958</td></tr><tr><td>Validation</td><td>RMSE</td><td>269.8</td><td>44.4</td><td>71.6</td></tr><tr><td></td><td>$ACC_{1\%}$</td><td>0.011</td><td>0.072</td><td>0.375</td></tr><tr><td></td><td>$ACC_{5\%}$</td><td>0.054</td><td>0.357</td><td>0.752</td></tr><tr><td></td><td>$ACC_{10\%}$</td><td>0.101</td><td>0.666</td><td>0.851</td></tr></table>
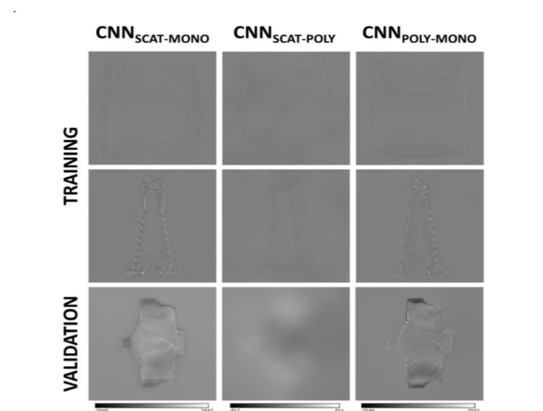

Figure 6 : Error between actual and estimated scatter and/or beam hardening maps, for the scan objects shown in the first, third, and fifth row of Figure 2. Negative grey values depict overestimation by the CNN model.</td></tr>
<tr><td>2018 Park et al. CT sinogram-consistency learning for metal-induced beam hardening correction</td><td></td><td>U-Net(CNN) from Ronnenberger et al. (2015)
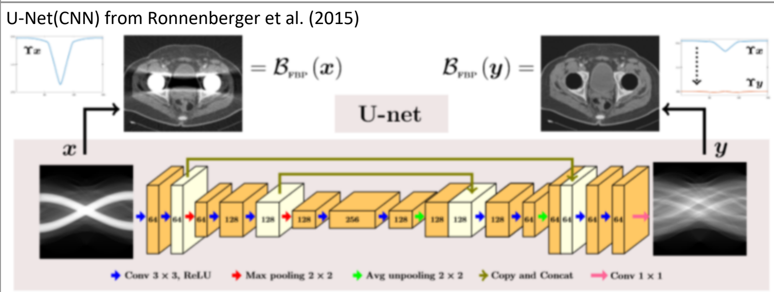
</td><td>• Patient-specific learning approach
  • Simulated data for training
  • Real-data for validation
  • Train domain different then test domain (pelvis)
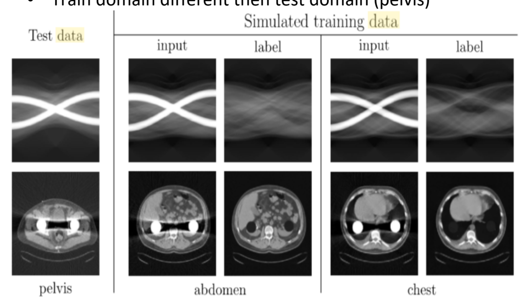
</td><td>• Train data:
  • 3780 CT sinogram data size 368x180
  • Images from 2 metallic objects chaning size and position
  • 80 validation images
  • 3700 train iamges</td><td>-</td><td>Parallel beam geometry</td><td>500</td><td>32</td><td>RMSPropOptimizer</td><td>Normalized root mean square differnece (NRMSD)</td><td>Lr = 0.001
Weight decay: 0.9</td><td>16 hours with tensorflow on 4x NVIDIA GTX-1080 8GB</td><td>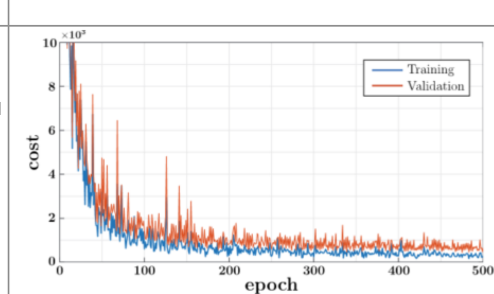

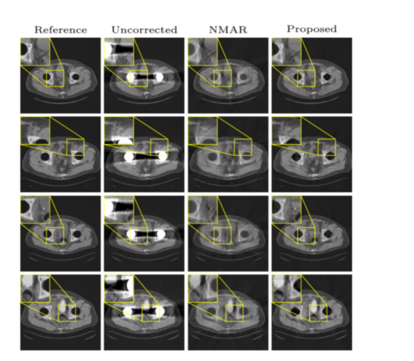

FIG. 7. Reconstruction results for pelvic CT images containing two simulated hip prostheses (made of iron). First and second columns show the reference and uncorrected image, respectively. The third and fourth columns represent the results with NMAR and the proposed method, respectively. First, second, third and fourth rows show results of variations of metal geometries with different tissue backgrounds. (C=-250 HU/W=2500 HU.)</td></tr>
<tr><td>2018, Zhou</td><td></td><td>64/32/1 is the number of convolution kernels
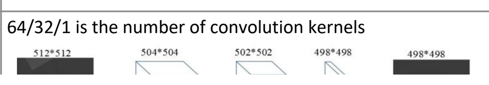
</td><td>• Noisy/ BH-data is created through real prallel beam geometry CT
• Ground truths are obtained through simulation of the basic shapes</td><td>• Slices reconstructe</td><td>Mono materia</td><td>No / Parallel</td><td></td><td></td><td>Stochastic</td><td>Euclidean distance between the artifact corrected image and ground truth</td><td>Lr = 0.0000</td><td>18h (NVIDI</td><td></td></tr>
</table>

et al. DL based beam hardening reduction

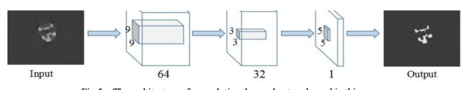

Fig.5 The architecture of convolutional neural network used in this paper.

- Layers can be seen as feature extraction
- Non-linear filtering
- Feature combination

First layer: $f_1(x) = \mathrm{ReLU}(\boldsymbol{W}_1 * x + \boldsymbol{b}_1)$ (3)

Second layer: $f_2(x) = \mathrm{ReLU}(\boldsymbol{W}_2 * x + \boldsymbol{b}_2)$ (4)

Third layer: $f_3(x) = \boldsymbol{W}_3 * x + \boldsymbol{b}_3$ (5)

They say there amount of layers is enough

Shapes: Circles, Squares, rectangles of different size and distance

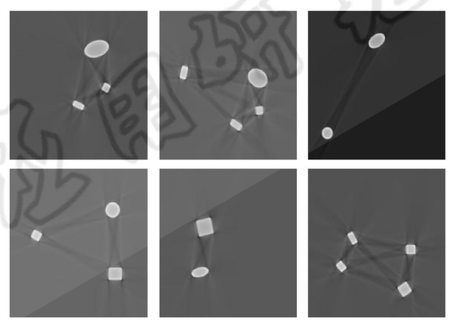

Fig.12 Some input images to train the network

d by FDK algorithm are the inputs
- Artifact free images reconstructed at fixed energies are the output
- Noisy/ BH-data is created through real prallel beam geometry CT
  - 400 Images per voltage (3 voltages)
    - 370 train / 30 test set
  - 1100 train and 90 test images
- Ground truths are obtained through simulation of the basic shapes
- No downsampling

l (Copper)

beam geometry

gradient decent

1

A GTX TITAN X)

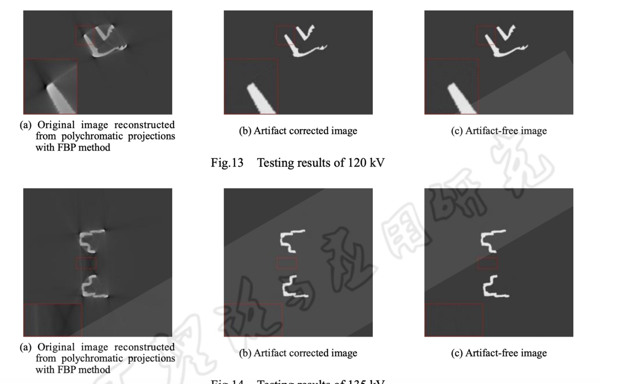
(a) Original image reconstructed from polychromatic projections with FBP method (b) Artifact corrected image (c) Artifact-free image

Fig.13 Testing results of 120 kV

(a) Original image reconstructed from polychromatic projections with FBP method (b) Artifact corrected image (c) Artifact-free image

Fig.14 Testing results of 135 kV

What is a sinogram in CT?

A sinogram is a **special x-ray procedure that is done to visualize any abnormal opening (sinus) in the body**, following the injection of contrast media (x-ray dye) into the opening. 2. ... An x-ray technologist will assist.

2019, Ziabari et al. X-Ray CT Reconstruction

his paper does focus more on X-CT-Reconstruction. They show here an approach with a DL-MBIR Network through which they reduce the time needed for reconstruction a lot

DL-MBIR Network through which they reduce the time needed for reconstruction a lot

Die Entscheidung das AI-CT model und den zugehörigen approach von 2020, Ziabari et al. Beam Hardening artifact reduction zu nutzen wurde getroffen, weil:

- Das Model mit Slices arbeitet und nicht mit Projections
- Es auf Beamhardening spezialisiert ist
- Es einen 2.5D approach nutzt (5 Slices geben ein Output Slice) (Korrelationen zwischen benachbarten Slices werden berücksichtigt)
- Es mit sehr wenig Daten trainiert wurde (6-CT Volumen)
- Die Architektur dann doch sehr einfach aussieht ---> 15/17 aneinander geschichtete CNN Layer
- Löcher/ Risse bleiben im Netz erhalten
- Die Resultate (SNR) sehen vielversprechend aus

CAD-data + MBIR Algorithm / FBP Algorithm (Fully simulated data)

	FBP	MBIR	2.5D DL-MBIR
PSNR (dB)	24.24	53	51.23
Computational Time (s)	5.6	3060	6.7

2018, Ziabari 2.5D DEEP LEARNING FOR CT IMAGE RECONSTRUCTION USING A MULTI-GPUIMPLEMENTATION

This Paper explains the DL-MBIR network which takes the FDK slices and makes out of them the MBIR slices. Also fully focused on 3D reconstruction

This Paper explains the DL-MBIR network which takes the FDK slices and makes out of them the MBIR slices.

Trained on existing clinical data

Deep scatter estimation (DSE): accurate real-time scatter estimation for x-ray CT using a deep convolutional neural network

Is about Scatter estimation: propose the deep scatter estimation (DSE). It uses a deep convolutional neural network which is trained to reproduce the output of MC simulations using only the acquired projection data as input. Thus, the accuracy of the scatter prediction should be comparable to MC simulations but can be generated in real-time once the network is trained.

The network consists of a downward path that plays a role at extracting a hierarchy of features from the input image and an upward path that restores the resolution of the image while transforming the features.

Fig. 1 Architecture of the proposed deep convolutional neural network

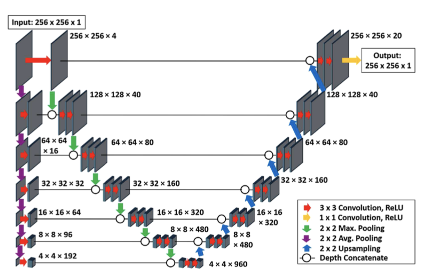

- The output of the Network is the scatter distribution which can then be subtracted from the images

- They use a Cad simulation approach with physical equations but they do not explain how they add the scatter + the poission noise which is calculated through the equations to the CAD data.

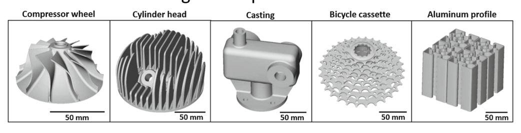

Fig. 2 Models used for the simulation study. The materials were chosen to be aluminum (cylinder head, casting, profile), steel (bicycle cassette) and a titanium alloy (compressor wheel). Note that the aluminum profile was used for testing only

follows. For each component primary intensities ψ were generated using an analytic model:

$$\psi(\boldsymbol{u}) = \frac{\int dE\, w(E)\, e^{-\mu(E)\cdot p(\boldsymbol{u})}}{\int dE\, w(E)}, \tag{6}$$

where $w(E)$ is the detected X-ray spectrum that was generated according to the model of Tucker et al. [35], $\mu(E)$ is the attenuation coefficient of the component according to the evaluated photon data library [4] and $p(\boldsymbol{u})$ is the intersection length at detector position $\boldsymbol{u}$ that is derived by a forward projection of the component's CAD model. Subsequently, X-ray scatter I_s was simulated using our in-house MC simulation [1]. Finally, Poisson noise $\mathcal{P}$ was added to generate the intensity data $\tilde{\psi}$:

$$\tilde{\psi}(\boldsymbol{u}) = \psi(\boldsymbol{u}) + I_s(\boldsymbol{u}) + \mathcal{P}(\psi(\boldsymbol{u}) + I_s(\boldsymbol{u})). \tag{7}$$

Trained on projection data:

Data is downsampled to 256x256

How much data:
- 16,416 projections were generated using the CAD model of a compressor wheel, a cylinder head, a casting and a bicycle cassette as prior (Fig. 2).
- The testing data set consists of a tomography (720 projections/360◦) of a compressor wheel, a cylinder head, a casting and a bicycle cassette and an aluminum profile with different simulation parameters as for the train set

- The labels are the output of a scatter distribution using a Monte Carlo (MC) Photon transport code

Mono material (only Aluminium)

Test were performed on a table-top CT (But everything should be applicable to a Cone-beam geometry)

80

16

Adam

Mean squared error between output and MC Scatter

GeForce GTX 1080

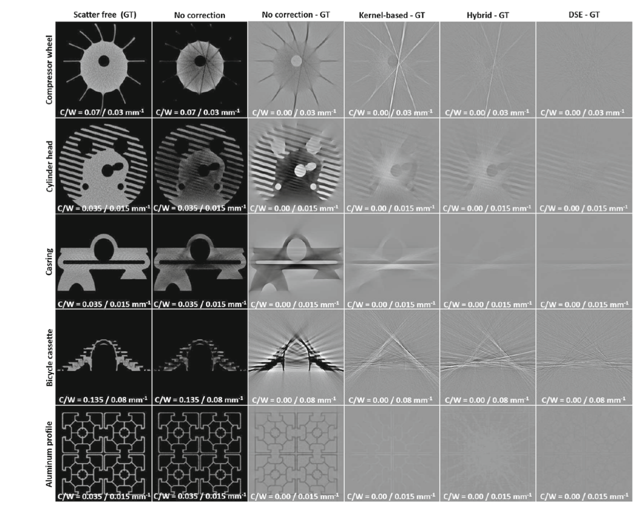
Fig. 5 CT reconstructions of projections without scatter (first column), with scatter (second column) as well as the difference between the scatter corrected reconstructions and the ground truth (third to sixth column)

Table 3 Mean and maximum absolute percentage error between the scatter estimate and the ground truth evaluated for all 720 projection views of each component

	Kernel-based		Hybrid		DSE	
	Mean	Max	Mean	Max	Mean	Max
Compressor wheel	19.8	84.0	11.7	61.6	1.46	13.2
Cylinder head	12.4	66.8	7.2	36.5	0.63	10.7
Casting	9.0	57.8	3.9	29.0	0.58	9.9
Bicycle cassette	13.3	87.7	8.5	63.4	0.66	12.1
Aluminum profile	8.8	30.3	2.7	16.4	0.78	5.0

Note, that the evaluation was restricted to the area of the component. The absolute percentage error in air was not considered since it does not affect the CT value accuracy of the reconstruction of the component

- The ground truth are the output of a scatter distribution using a Monte Carlo (MC) Photon transport code

---

Reduction of metal artifacts in x-ray CT images using a convolutional neural network

(2020), Yanbo Zhang et. all

(Convolutional Neural Network based Metal Artifact Reduction in X-ray Computed

- Works on slices & Projections
- Uses a lot of pre & post processing
- We could take from this method the idea: to take as an input also pre corrected images of classical methods.

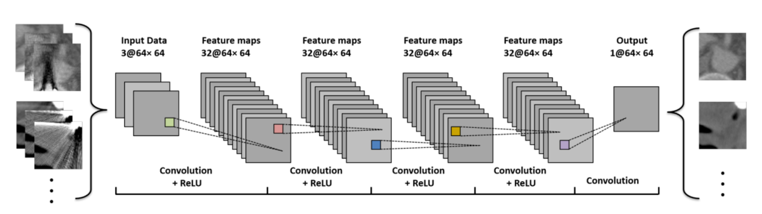

Figure 3. Configuration of the convolutional neural network for metal artifact reduction.

CNN, which is comprised of an input layer, an output layer and L = 5 convolutional layers. ReLU, a nonlinear activation function defined as ReLU(x) = max(0; x), is performed after each of the first L ¡ 1 convolutional layers.

They do much more preprocessing & Post-processing:

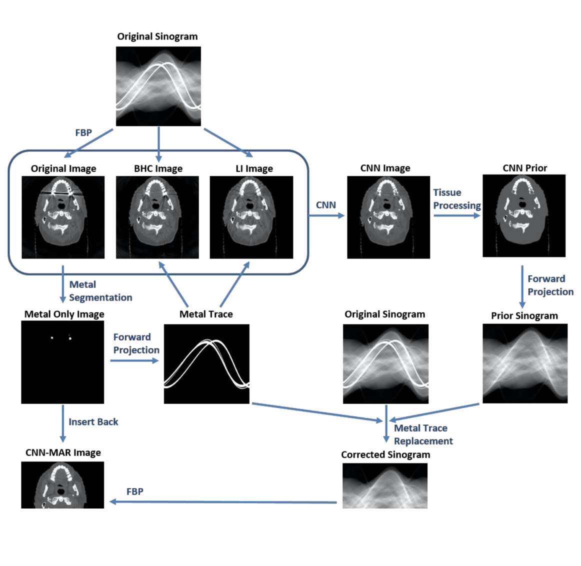

Selve made slimualtion & approximations :

They create a database with:
- metal-free images,
- metal-inserted,
- and MAR methods processed images

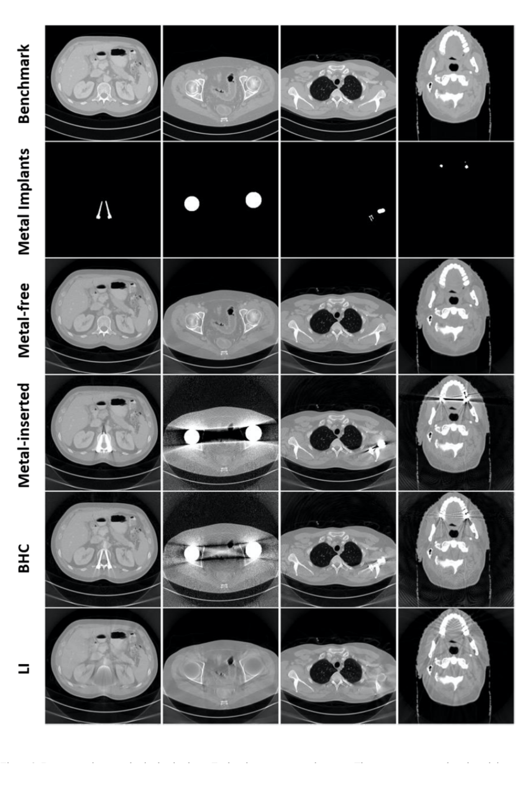

sample in the database: 3-Channel Image:
- original uncorrected image
- BHC image
- LI image

input data of CNN :
- image patches of s×t×3 are extracted from three-channel images,

water(tissue, water similar), bone and metals

fan-beam geometry

these patches are assumed as the target of CNN during training. The r^{th} training sample pair is denoted as $\mathbf{u}_r \in \mathbb{R}^{s\times t\times 3}$ and $\mathbf{v}_r \in \mathbb{R}^{s\times t}$, $r = 1, \ldots, R$, where R is the number of training samples. The CNN training is to find a function $H : \mathbb{R}^{s\times t\times 3} \to \mathbb{R}^{s\times t}$ that minimizes the following cost function [24]:

$$H = \arg\min_H \frac{1}{R}\sum_{r=1}^{R} \|H(\mathbf{u}_r) - \mathbf{v}_r\|_F^2, \tag{1}$$

where $\|\cdot\|_F$ is the Frobenius norm.

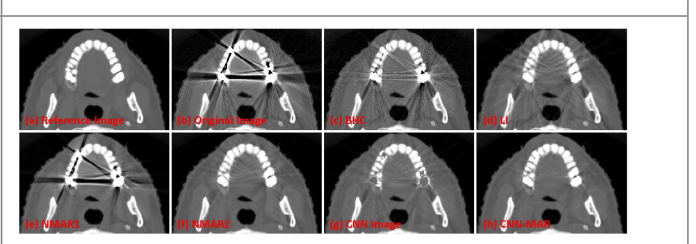

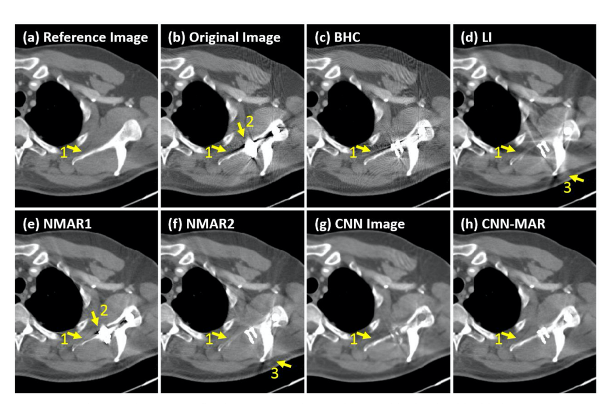

Figure 9. Case 2: two fixation screws and a metal inserted in the shoulder blade.

Tomography (2018), is the previous work & the same network)		Figure 4. Illustration of the proposed CNN-MAR method. **2.3 CNN-MAR Method** Because the proposed MAR approach is based on CNN, it is referred as to CNN-MAR method. It consists of five steps: (1) metal trace segmentation; (2) reduce artifacts with LI and BHC; (3) reduce artifacts with the trained CNN; (4) generate a CNN prior image using tissue processing; (5) replace metal affected projections with the forward projection of CNN prior, followed by the FBP reconstruction. The workflow of CNN-MAR is summarized in Fig. 4. Steps 1 and 5 are the same to our previous work [21], and step 2 has been described in the above subsection. Hence, we only state the key steps 3 and 4 as follows. They replace metal affected projections with forward projections of the CNN prior (Get this through tissue preprocessing)	Figure 2. Representative samples in the database. Each column corresponds a case. The top two rows are benchmark images and metal-only images, respectively. The third and fourth rows are metal-free and metal-inserted images, respectively. The last two rows are images after metal artifact reduction using BHC and LI, respectively. We apply two simple metal artifact reduction methods, the linear interpolation (LI) and beam hardening correction (BHC) proposed in [30]										
Metal artifact reduction in computed tomography images based on developed generative adversarial neural network (2021)	GAN-approach with UNET based generator.	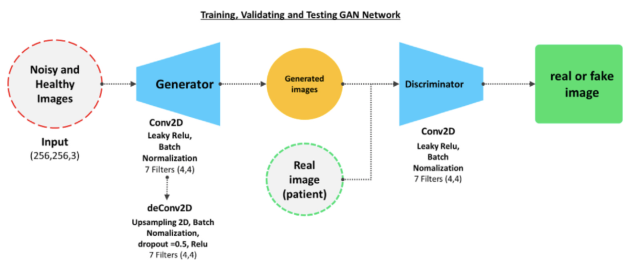 **Fig. 2.** GAN architecture.											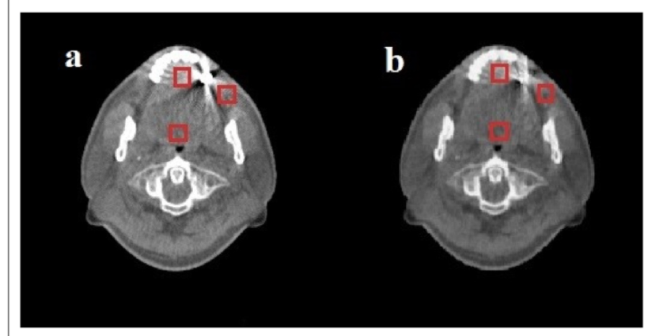
DuDoNet: Dual Domain Network for CT Metal Artifact Reduction													
Fast Enhanced CT Metal Artifact Reduction Using Data Domain Deep Learning													
Distraction-aware Shadow Detection	Maybe copy approaches from shadow removal												